

Weyl points in a magnetic tetrahedral photonic crystal

ZHAOJU YANG,¹ MENG XIAO,² FEI GAO,¹ LING LU,³ YIDONG CHONG,^{1,4,5}
AND BAILE ZHANG^{1,4,6}

¹*Division of Physics and Applied Physics, School of Physical and Mathematical Science, Nanyang Technological University, Singapore 639798, Singapore*

²*Department of Electrical Engineering, and Ginzton Laboratory, Stanford University, Stanford, California 94305, USA*

³*Institute of Physics, Chinese Academy of Sciences/Beijing National Laboratory for Condensed Matter Physics, Beijing 100190, China*

⁴*Centre for Disruptive Photonic Technologies, Nanyang Technological University, Singapore 637371, Singapore*

⁵*yidong@ntu.edu.sg*

⁶*blzhang@ntu.edu.sg*

Abstract: Weyl points have recently been predicted and experimentally observed in double-gyroid photonic crystals, as well as in other complex photonic structures such as stacked hexagonal-lattice slabs and helical waveguide arrays. In all above structures, the Weyl points are located between high frequency bands, and are difficult to probe experimentally. In this work, we show that a photonic crystal with a simple tetrahedral structure can host frequency-isolated Weyl points between the second and third bands. The minimal number of two Weyl points emerges from a threefold quadratic degeneracy at the Brillouin zone corner when time-reversal symmetry is broken. We verify theoretically that the Weyl points carry opposite topological charges, and are associated with Fermi arc-like surface states. This photonic crystal can be realized using ferromagnetic rods in the microwave frequency regime, providing a simple platform for studying the physics of Weyl points.

© 2017 Optical Society of America

OCIS codes: (350.1370) Berry's phase; (000.1600) Classical and quantum physics; (050.5298) Photonic crystals.

References and links

1. V. H. Weyl, "Elektron und Gravitation. I.," *Z. Phys.* **56** (1929).
2. X. Wan, A. M. Turner, A. Vishwanath, and S. Y. Savrasov, "Topological semimetal and Fermi-arc surface states in the electronic structure of pyrochlore iridates," *Phys. Rev. B* **83**, 205101 (2011).
3. B. Q. Lv, H. M. Weng, B. B. Fu, X. P. Wang, H. Miao, J. Ma, P. Richard, X. C. Huang, L. X. Zhao, G. F. Chen, Z. Fang, X. Dai, T. Qian, and H. Ding, "Experimental Discovery of Weyl Semimetal TaAs," *Phys. Rev. X* **5**, 031013 (2015).
4. S.-Y. Xu, I. Belopolski, N. Alidoust, M. Neupane, G. Bian, C. Zhang, R. Sankar, G. Chang, Z. Yuan, C.-C. Lee, S.-M. Huang, H. Zheng, J. Ma, D. S. Sanchez, B. Wang, A. Bansil, F. Chou, P. P. Shibayev, H. Lin, S. Jia, and M. Z. Hasan, "Discovery of a Weyl fermion semimetal and topological Fermi arcs," *Science* **349**(6248), 613–617 (2015).
5. L. Lu, L. Fu, J. D. Joannopoulos, and M. Soljačić, "Weyl points and line nodes in gyroid photonic crystals," *Nat. Photonics* **7**(4), 294–299 (2013).
6. L. Lu, Z. Wang, D. Ye, L. Ran, L. Fu, J. D. Joannopoulos, and M. Soljačić, "Experimental observation of Weyl points," *Science* **349**(6248), 622–624 (2015).
7. W. J. Chen, M. Xiao, and C. T. Chan, "Photonic crystals possessing multiple Weyl points and the experimental observation of robust surface states," *Nat. Commun.* **7**, 13038 (2016).
8. W. Gao, B. Yang, M. Lawrence, F. Fang, B. Béri, and S. Zhang, "Photonic Weyl degeneracies in magnetized plasma," *Nat. Commun.* **7**, 12435 (2016).
9. M. Xiao, W.-J. Chen, W.-Y. He, and C. T. Chan, "Synthetic gauge flux and Weyl points in acoustic systems," *Nat. Phys.* **11**(11), 920–924 (2015).
10. Z. Yang and B. Zhang, "Acoustic Type-II Weyl Nodes from Stacking Dimerized Chains," *Phys. Rev. Lett.* **117**(22), 224301 (2016).
11. J. Noh, S. Huang, D. Leykam, Y. D. Chong, K. Chen, and M. C. Rechtsman, "Experimental observation of optical Weyl points," arXiv 1610.01033 (2016).

12. J. Bravo-Abad, L. Lu, L. Fu, H. Buljan, and M. Soljačić, “Weyl points in photonic-crystal superlattices,” *2D Materials* **2**, 034013 (2015).
13. M. Xiao, Q. Lin, and S. Fan, “Hyperbolic Weyl Point in Reciprocal Chiral Metamaterials,” *Phys. Rev. Lett.* **117**(5), 057401 (2016).
14. L. Lu, J. D. Joannopoulos, and M. Soljačić, “Topological photonics,” *Nat. Photonics* **8**(11), 821–829 (2014).
15. F. D. Haldane and S. Raghu, “Possible realization of directional optical waveguides in photonic crystals with broken time-reversal symmetry,” *Phys. Rev. Lett.* **100**(1), 013904 (2008).
16. J. Y. Chin, T. Steinle, T. Wehler, D. Dregely, T. Weiss, V. I. Belotelov, B. Stritzker, and H. Giessen, “Nonreciprocal plasmonics enables giant enhancement of thin-film Faraday rotation,” *Nat. Commun.* **4**, 1599 (2013).
17. A. K. Zvezdin and V. A. Kotov, *Modern Magneto-optics and Magneto-optical Materials* (CRC Press, 1997).
18. J. P. Bouchaud and P. G. Zerah, “Spontaneous resonances and universal behavior in ferrimagnets: Effective-medium theory,” *Phys. Rev. Lett.* **63**(9), 1000–1003 (1989).
19. S. Johnson and J. Joannopoulos, “Block-iterative frequency-domain methods for Maxwell’s equations in a planewave basis,” *Opt. Express* **8**(3), 173–190 (2001).
20. A. A. Soluyanov, D. Gresch, Z. Wang, Q. Wu, M. Troyer, X. Dai, and B. A. Bernevig, “Type-II Weyl semimetals,” *Nature* **527**(7579), 495–498 (2015).
21. L. Lu, and Z. Wang, “Topological one-way fiber of second Chern number,” arXiv 1611, 01998 (2016).
22. A. Slobozhanyuk, S. H. Mousavi, X. Ni, D. Smirnova, Y. S. Kivshar, and A. B. Khanikaev, “Three-dimensional all-dielectric photonic topological insulator,” *Nat Photon advance online publication* (2016).

1. Introduction

Weyl points are the topological band degeneracies in three dimensions. They are governed by the Weyl Hamiltonian [1] $H(k) = \sum_{i,j=x,y,z} k_i v_{ij} \sigma_j$ (where k_i , v_{ij} and σ_j respectively denote the wave-vector, velocity and Pauli matrix). Originally proposed by Hermann Weyl to describe massless relativistic fermions [1], this Hamiltonian was recently found to occur in certain band structures possessing broken inversion (P) symmetry and/or broken time-reversal (T) symmetry; the band-crossing points, or “Weyl points”, carry topological charge and are robust against perturbations to the underlying lattice. Apart from condensed-matter realizations [2–4], Weyl Hamiltonians can also occur in classical wave systems, such as photonic crystals [5–8] and acoustic crystals [9,10]. Lu et al. predicted the existence of photonic Weyl points in a double-gyroid photonic crystal with broken P and/or T [5], and subsequently verified their existence for the P-broken case [6]. “Fermi arc-like” topological surface states associated with photonic Weyl points have been observed in a P-broken photonic crystal consisting of stacked hexagonal lattice slabs [7], and “type-II” Weyl points and their surface states have been observed in an array of helical optical waveguides [11]. Other structures that have been predicted to host Weyl points include stacked triangular photonic crystal slabs [12], arrays of helical metal wires [13], and stacked acoustic resonator chains [9,10].

Here, we show that Weyl points can occur in a photonic crystal based on a tetrahedral lattice of space group 208. The structure, shown in Fig. 1(a), appears to be considerably simpler than the ones employed in previous studies (double-gyroid, stacked slabs, etc.) [7,12,14]. The unit cell is cubic, and contains four cylindrical rods. The lattice inherently lacks P symmetry. So long as T symmetry is unbroken, its band structure lacks Weyl points, instead exhibiting a threefold quadratic degeneracy at the corner of the Brillouin zone. However, when T is broken by applying gyroelectric anisotropy (e.g., by constructing the rods out of ferromagnetic materials [5,15–17], such as bismuth iron garnet - a rare-earth garnet with ferromagnetically ordered domains), the degeneracy is lifted to produce a pair of well-isolated Weyl points with opposite chiralities (Berry fluxes). We show also that the photonic crystal exhibits the expected Fermi arc-like surface states. This design may thus provide a simple route for fabricating photonic crystals with Weyl modes.

2. Tetrahedral photonic crystal

In the photonic crystal’s unit cell, shown in Fig. 1(a), the four dielectric rods (shown in gold) are centered at $(0.25, 0.25, 0.25)a$, $(-0.25, -0.25, 0.25)a$, $(0.25, -0.25, -0.25)a$ and $(-0.25,$

$0.25, -0.25)a$, where a is the length of each side of the cubic cell. The rod axes point from the center of the cubic cell towards $[1,1,1]$, $[-1, -1, 1]$, $[1, -1, -1]$, and $[-1, 1, -1]$ respectively. The lattice forms the space group 208, and evidently does not possess inversion symmetry P . The first Brillouin zone, shown in Fig. 1(b), is cubic. We fix the rod radius as $r = 0.13a$, and initially take the rod material to be an ordinary dielectric with permittivity $\epsilon = 16$. The magnetic permeability is unity everywhere [5,18], and the rest of the volume is air.

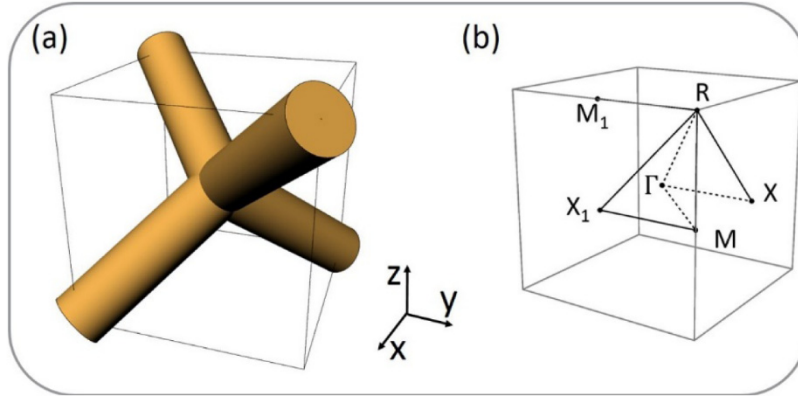


Fig. 1. Unit cell of the tetrahedral photonic crystal and Brillouin zone. (a) The unit cell consists of four rods of radius $r = 0.13a$. The rods point from $(0, 0, 0)$ to $(0.5, 0.5, 0.5)$, $(-0.5, -0.5, 0.5)$, $(0.5, -0.5, -0.5)$, $(-0.5, 0.5, -0.5)$, respectively. (b) The cubic Brillouin zone of space group 208.

Figure 2(a) shows the photonic band structure along high symmetry lines of the first Brillouin zone. At the Brillouin zone corner $R = (0.5, 0.5, 0.5)$ (in unit of $2\pi/a$), the lowest three bands meet at a threefold quadratic degeneracy at frequency $0.351 \times 2\pi c/a$ (where c is the speed of light). This is reminiscent of the threefold degeneracy in the band structure of the double-gyroid photonic crystal studied in Ref [5], which can be lifted to produce Weyl points by breaking either P or T . In the present structure, the underlying lattice already lacks P , so we resort to breaking T by magnetizing the rods along the y direction to induce a gyroelectric response. The dielectric tensor in the rods now acquires nonzero off-diagonal imaginary components [5,15,17],

$$\epsilon = \begin{pmatrix} \epsilon_{xx} & 0 & i\kappa \\ 0 & \epsilon_{yy} & 0 \\ -i\kappa & 0 & \epsilon_{zz} \end{pmatrix}.$$

We take $\epsilon_{yy} = 16$, $\epsilon_{xx} = \epsilon_{zz}$, $\kappa = 10$ and $\epsilon_{xx}^2 - \kappa^2 = \epsilon_{yy}^2$, consistent with gyroelectric materials. Note that T -breaking can be implemented equally well via μ for gyromagnetic materials. Therefore ferrimagnetic materials with a gyromagnetic response give the same results.

The band structure of the magnetized photonic crystal is shown in Fig. 2(b). The threefold quadratic degeneracy is lifted, and we observe a linear band-crossing point between the second and third bands, located along the Brillouin zone's RM_1 symmetry line, at frequency $0.374 \times 2\pi c/a$. This is one of a pair of Weyl points; the other one lies along the same symmetry line, but at the opposite side of the first Brillouin zone, as shown in Fig. 2(c). The two bands are joined by exactly two Weyl points, the minimum number that can exist in Weyl crystals (which can only occur in T -broken crystals) [14]. Figure 3(a) shows the linear band dispersion in the vicinity of the Weyl point at $k = (0.50, 0.31, 0.50)$.

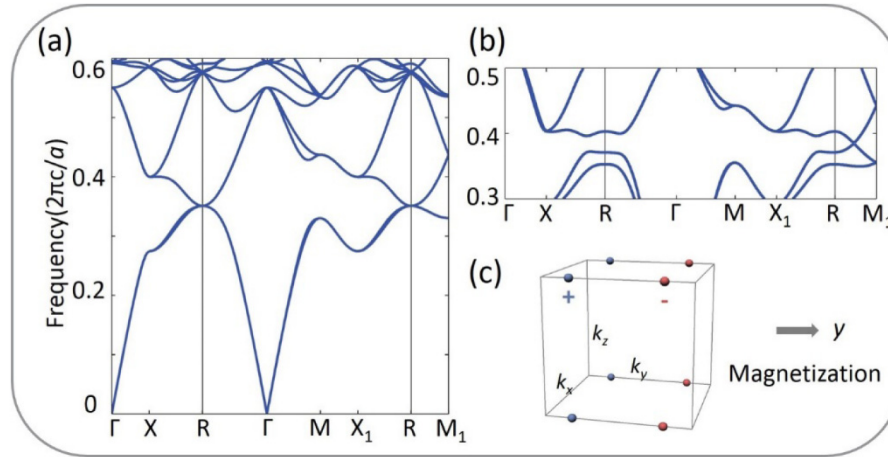


Fig. 2. Band structure of the photonic crystal with and without magnetization. (a) Band structure without magnetization. (b) Band structure with magnetization along y direction. (c) The distribution of the Weyl point in the first Brillouin zone. Red and Blue points represent Weyl points with opposite chirality.

3. Weyl points and one-way surface state

To verify that the linear band-crossing points are indeed Weyl points, we numerically calculate their topological charge (chirality). Starting from the frequency-domain Maxwell equations, the electric field is eliminated to obtain the second-order master equation

$$\nabla \times \frac{1}{\varepsilon(r)} \nabla \times H(r) = \left(\frac{\omega}{c} \right)^2 H(r) \quad \text{where } H \text{ is the magnetic field and } \omega \text{ is the angular}$$

frequency. We take Bloch functions $H(r) = u_{n,k}(r) \exp(ik \cdot r)$, where n is the band index; the cell periodic functions $u_{n,k}$ obey the orthonormality condition

$$u_{n,k}(r) |u_{n',k}(r) = \int u_{n,k}(r) u_{n',k}(r) d^3r = \delta_{n,n'}$$

with the integral taken over the unit cell. The Bloch functions and eigenfrequencies are computed using the MPB software package [19]. The topological charge of each Weyl point is then calculated by the numerical method described in Refs [20]. The Weyl point is enclosed by a sphere of k -space radius $0.05 \times 2\pi/a$, parameterized by the polar angle θ and azimuthal angle ϕ , as shown in Fig. 3(b). For each closed loop of constant θ_i , the Berry phase is computed using the discretized formula

$$\gamma_n = -\text{Im} \ln \prod_j u_{n,k_j} |u_{n,k_{j+1}}$$

where k_j represents j th point along the loop. These Berry phases are plotted versus θ ; the results, for the three lowest bands and for the Weyl point at $k = (0.50, 0.31, 0.50)$, are shown in Fig. 3(c). As we vary θ from 0 to π , the Berry phase of the first band remains zero, whereas the Berry phase of the second (third) band changes continuously from 2π to 0 (from 0 to 2π). Note that the Berry phase can only be an integer multiple of 2π when θ varies from 0 to π . The result of such a calculation is equivalent to taking the surface integral of the Berry curvature over a closed surface. Therefore, this integer multiple is equal to the monopole charge enclosed and gives the chirality of the Weyl point enclosed. We conclude that this Weyl point at $k = (0.50, 0.31, 0.50)$ carries a topological charge (Chern number) of -1 [20]. Repeating the calculation for the other Weyl point, its topological charge is found to be $+1$, as expected.

The topological features of Weyl points imply the existence of protected surface states, referred to as ‘‘Fermi arc surface states’’ in the condensed-matter context [2]. We look for surface states by taking a 3D photonic crystal slab that is finite in the z direction and infinite

in the x and y directions. In this case, k_x and k_y are good quantum numbers, and the Weyl nodes are projected along the k_z direction, as indicated by the blue and red dots in Fig. 3(e). In calculating Fig. 3(d)–(e), the claddings consisting of single gyroid photonic crystals with band gaps near the frequency range of the Weyl points are added on the top and bottom of the supercell, in order to confine the electromagnetic waves. In Fig. 3(d), we plot the projected band structure as a function of k_x , with fixed $k_y = 0.5 \times 2\pi/a$. We observe a dispersion curve (the red line), representing surface states localized to one surface (the dispersion curve for states on the opposite surface is suppressed). Note that the group velocity flips sign within a very small frequency range around $0.38 \times 2\pi c/a$; this behavior is dependent on boundary details and does not violate the bulk-edge correspondence principle. This is up to the trivial materials we adopted in simulations. In Fig. 3(e), we trace out the locus of surface states in the two-dimensional (k_x - k_y) Brillouin zone, at fixed frequency $0.366 \times 2\pi c/a$. This locus forms an open arc connecting the projected positions of the two Weyl points, similar to the “Fermi arcs” that have been predicted and observed in Weyl semi-metals [2–4]. (Here, the chosen operating frequency plays the role of the Fermi level).

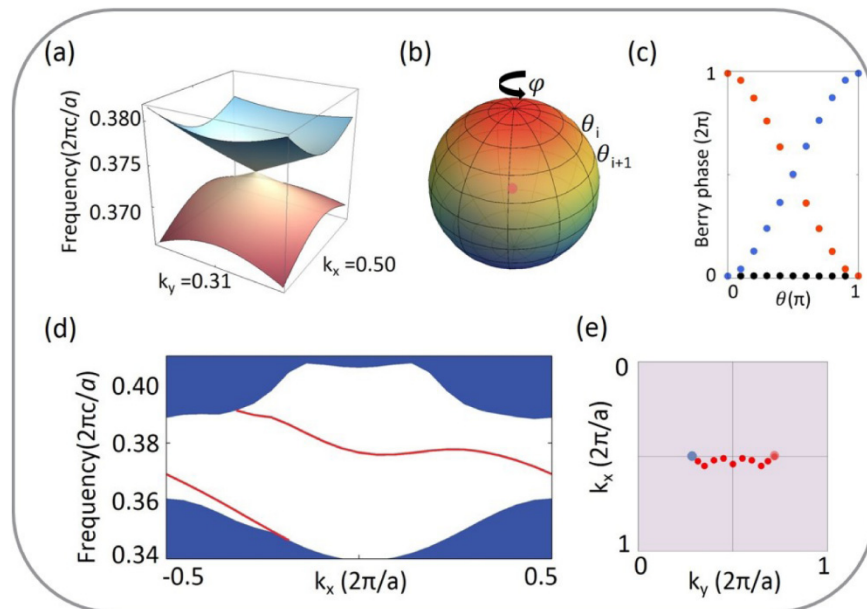


Fig. 3. The chirality and topological surface states. (a) The band structure in vicinity of the Weyl point at $(0.50, 0.31, 0.50)$ with $k_z = 0.5$. The frequency of degeneracy is $0.374 \times 2\pi c/a$. (b) The sphere in momentum space enclosing one Weyl point. The radius of the sphere is $0.05 \times 2\pi/a$. (c) The calculated Berry phase as a function of polar angle. The center of the sphere locates at the Weyl point $(0.50, 0.31, 0.50)$. (d) The topologically protected surface state. (e) The photonic open arc (dark red dotted line) traced out from surface states at the fixed frequency $0.366 \times 2\pi c/a$ in the surface Brillouin zone centered at R point.

4. Conclusion and discussions

In conclusion, we have shown that a photonic crystal with a simple tetrahedral structure can exhibit Weyl points when T symmetry is broken via gyro-electric anisotropy. The tetrahedral lacks P symmetry, but without T breaking the band structure contains only a threefold quadratic degeneracy at the Brillouin zone corner; breaking T lifts this degeneracy and produces a pair of Weyl points between the second and third bands. We have verified that the Weyl points carry topological charge (chirality), and that they are associated with topologically-protected Fermi-arc-like photonic surface states. This photonic crystal can be realized at microwave frequencies by using ferromagnetic rods [17] with internal remnant

magnetization, which would not have to be biased using an external magnetic field. This may offer a new platform for exploring the rich physics of Weyl modes and other 3D photonic topological phases [21,22].

Funding

Nanyang Technological University under NAP Start-Up Grant; Singapore Ministry of Education under Grant No. MOE2015-T2-1-070, Grant No. MOE2011-T3-1-005; Singapore National Research Foundation under Grant No. NRFF2012-02; Singapore MOE Academic Research Fund Tier 2 Grant No. MOE2015-T2-2-008. L.L. was supported by the Ministry of Science and Technology of China under Grant No. 2017YFA0303800, 2016YFA0302400 and the National Thousand Young Talents Program of China.

Weyl points in a magnetic tetrahedral photonic crystal: erratum

ZHAOJU YANG,¹ MENG XIAO,² FEI GAO,¹ LING LU,³ YIDONG CHONG,^{1,4,5}
AND BAILE ZHANG^{1,4,6}

¹*Division of Physics and Applied Physics, School of Physical and Mathematical Sciences, Nanyang Technological University, Singapore 639798, Singapore*

²*Department of Electrical Engineering, and Ginzton Laboratory, Stanford University, Stanford, CA 94305, USA*

³*Institute of Physics, Chinese Academy of Sciences/Beijing National Laboratory for Condensed Matter Physics, Beijing 100190, China*

⁴*Centre for Disruptive Photonic Technologies, Nanyang Technological University, Singapore 637371, Singapore*

⁵*yidong@ntu.edu.sg*

⁶*blzhang@ntu.edu.sg*

Abstract: We present an erratum regarding the number of space group in our paper.

OCIS codes: (350.1370) Berry's phase; (000.1600) Classical and quantum physics; (050.5298) Photonic crystals.

References and links

1. Z. Yang, M. Xiao, F. Gao, L. Lu, Y. Chong, and B. Zhang, "Weyl points in a magnetic tetrahedral photonic crystal," *Opt. Express* **25**(14), 15772–15777 (2017).
2. S. Meiboom, M. Sammon, and W. F. Brinkman, "Lattice of disclinations: The structure of the blue phases of cholesteric liquid crystals," *Phys. Rev. A* **27**(1), 438–454 (1983).
3. S. Meiboom, M. Sammon, and D. W. Berreman, "Lattice symmetry of the cholesteric blue phases," *Phys. Rev. A* **28**(6), 3553–3560 (1983).

We have found that the correct space group of the photonic crystal in our main text [1] is 224 [The incorrect 'space group 208' appears at paragraph 2, page 2 and paragraph 1, page 3]. It has inversion symmetry, as can be seen in Fig. 1 with a different origin changing from (0, 0, 0) to (1/4, 1/4, 1/4)a. The results in our paper are still valid. We note that its space group was incorrectly identified as 208, as in [2-3] of liquid crystals.

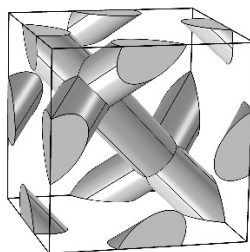


Fig. 1. The unit cell of space group 224 with inversion symmetry.